Investigation of the aerodynamics of an innovative vertical-axis wind turbine

Journal of Physics: Conference Series **530** (2014) 012007 doi:10.1088/1742-6596/530/1/012007

Investigation of the aerodynamics of an innovative vertical-axis wind turbine

K Kludzinska[1], K Tesch[1,3] and P Doerffer[2]
[1]Gdansk University of Technology, ul. G.Narutowicza 11/12, 80-233, Gdansk, Poland
[2]Institute of Fluid Flow Machinery, ul. Fiszera 14, 80-231, Gdansk, Poland

E-mail: krzyte@pg.gda.pl

Abstract. This paper presents a preliminary three dimensional analysis of the transient aerodynamic phenomena occurring in the innovative modification of classic Savonius wind turbine. An attempt to explain the increased efficiency of the innovative design in comparison with the traditional solution is undertaken. Several vorticity measures such as enstrophy, absolute helicity and the integral of the velocity gradient tensor second invariant are proposed in order to evaluate and compare designs. Discussed criteria are related to the vortex structures and energy dissipation. These structures are generated by the rotor and may affect the efficiency. There are also different vorticity measure taking advantage of eigenvalues of the velocity gradient tensor.

1. Introduction

The object of the analysis is the modernisation of classic design of the turbine (i.e. the Savonius wind turbine), see figure 1. This innovative design [1] is equipped with a stator which experimentally shows increased efficiency in comparison with standard design. This is true for wind tunnel experiments at least. Both turbines have the simplest design of all devices converting wind into other energy forms, which provides an opportunity for decrease of its price. The original Savonius wind turbine has numerous advantages such as low noise, simplicity of design, applicability for a wide range of wind velocities. The biggest problem of the classic design is its relatively low efficiency. The innovative design, discussed here, is devoid of this disadvantage.

Wind turbine research, such as Savonius turbine and its modifications, are in line with the general strategy of development of the Polish power industry. This strategy tends to quantitative increase the use of renewable energy sources. One of the limits, as far as the wind energy is concerned, it is high price of wind turbines available. The obtained results may increase the knowledge of the flow round a whole family of different types of rotors whose principle of operation is based primarily on the use of wind thrust accompanied with a small share of lift forces. The knowledge gained during the simulations will enable more effective designs characterised by increased efficiency and operational reliability.

The flow inside the rotor is complicated and that is why in past investigations were limited only to laboratory tests [2, 3, 4]. Another experimental method was flow visualisation [5, 6], which allows capturing flow patterns characteristics for selected instantaneous positions of rotor blades with respect

[3] To whom any correspondence should be addressed.

to the wind direction. Recently, due to the rapid development of computer hardware and software, attempts were made to analyse the structure of the flow through the Savonius rotor numerically [7, 8]. This also includes the vortex method [9, 10]. Generally, all data presented on the numerical aspect are mostly two-dimensional. Also, papers on attempts to modify the shape of the Savonius rotor are available [3, 11]. The best shapes of blade tips for a given rotor geometry and physical conditions are investigated in [12, 13, 14].

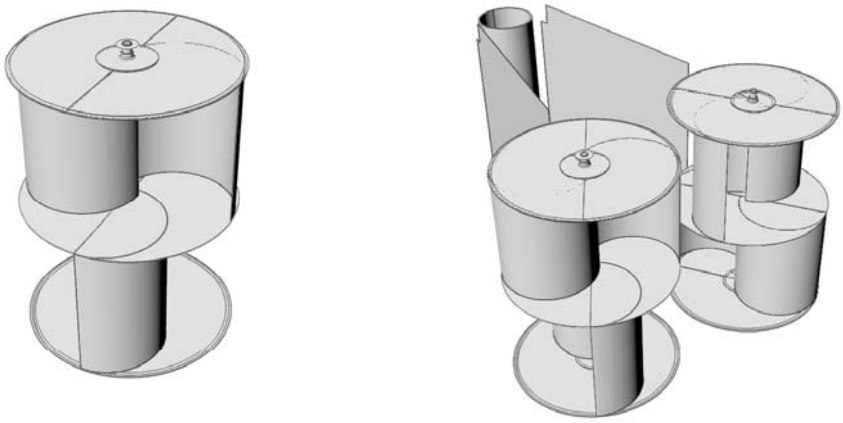

Figure 1. Classic (left) and innovative (right) designs.

2. Methodology

All the numerical calculations were performed using the commercial CFD code CFX. The turbulent flow of air was treated as an incompressible medium. The turbulence was modelled by means of the standard two-equation turbulence model $k-\varepsilon$. The reason for this choice may be explained by a need of comparison with other calculations found elsewhere. The $k-\varepsilon$ model has now become a standard for this kind of calculations.

The average form of mass conservation equation has the form

$$\nabla \cdot \left\langle \vec{U} \right\rangle = 0. \tag{1}$$

The Reynolds equation is

$$\rho \frac{\mathrm{d}\left\langle \vec{U} \right\rangle}{\mathrm{d}t} = \rho \vec{g} - \nabla p_{\mathrm{e}} + \nabla \cdot \left(2\mu_{\mathrm{e}} \left\langle \mathbf{D} \right\rangle\right) \tag{2}$$

where the effective pressure $p_{\mathrm{e}} = \left\langle p \right\rangle + 2\rho 3^{-1} k$ and the effective viscosity is composed of eddy and molecular components $\mu_{\mathrm{e}} = \mu_{\mathrm{t}} + \mu$. Two additional transport equations are those for modelled kinetic energy of velocity fluctuation k which arises from Reynolds stress transport equation

$$\rho \frac{\mathrm{d}k}{\mathrm{d}t} = 2\mu_{\mathrm{t}} \left\langle \mathbf{D} \right\rangle^2 + \nabla \cdot \left(\mu_{\mathrm{t}} \sigma_{\mathrm{k}}^{-1} \nabla k\right) - \rho\varepsilon \tag{3}$$

and dissipation of kinetic energy of fluctuation ε. This is analogous to k transport

$$\rho \frac{\mathrm{d}\varepsilon}{\mathrm{d}t} = C_{\varepsilon 1} \varepsilon k^{-1} 2\mu_{\mathrm{t}} \left\langle \mathbf{D} \right\rangle^2 + \nabla \cdot \left(\mu_{\mathrm{t}} \sigma_{\varepsilon}^{-1} \nabla \varepsilon\right) - \rho C_{\varepsilon 2} \varepsilon^2 k^{-1}. \tag{4}$$

The eddy viscosity is defined as $\mu_t = C_\mu \rho k^2 \varepsilon$. The five constants in the above equations should be deduced from experiment for a specific geometry. This 'standard' set is given by $\sigma_k = 1$, $\sigma_\varepsilon = 1$, $C_\mu = 0.09$, $C_{\varepsilon 1} = 1.44$, $C_{\varepsilon 2} = 1.92$.

The flow domain was divided into two parts: the rotating rotor and the steady wind tunnel and ambient. Both parts were merged by means of the domain interface of the so called 'transient rotor-stator' type. The time step of the transient calculations corresponded to two degree of revolution and the angular velocity of the rotating domain (rotor) corresponded to three turns per second.

The boundary conditions selected here are:

- Inlet. The mass flow rate was specified here. The specified mass flow rate corresponds to the average velocity $6\,\mathrm{m\,s^{-1}}$. The turbulence intensity defined as $\tau_t = \left\langle \vec{U} \right\rangle^{-1} \left(2k3^{-1}\right)^{1/2}$ equals 5% and the viscosity ratio $\mu_t \mu^{-1} = 10$. This represents a medium turbulent intensity.
- Opening. The so called 'far field' condition was chosen equal with prescribed constant atmospheric pressure.
- Symmetry. This means than the velocity normal component equals zero $\hat{n} \cdot \left\langle \vec{U} \right\rangle = \vec{0}$ and all the scalar values φ must fulfil $\hat{n} \cdot \nabla \varphi = 0$ where $\hat{n}$ represents a unit vector normal to the surface.
- Wall. The flow domain was a wind tunnel with one side open to the atmosphere. As for the rotor blades and the shroud they were modelled as no slip wall in the rotating frame of reference.

3. Coefficients

Among many characteristics of the wind turbines the most important is the torque coefficient. It is commonly defined as

$$C_T = \frac{T}{\frac{1}{4}\rho U^2 D^2 H}. \tag{5}$$

The above definition is valid for both the steady-state and transient flows. For the latter case one should use the time dependent torque $T(t)$ instead of T meaning that in real case we deal with the distribution of C_T as a function of the angular position of the rotor. The torque coefficient (5) is directly related to the efficiency of the rotor.

A typical definition of the efficiency for the steady-state case takes under consideration the wind power $N_w = \dot{m} e_k = \rho U S 2^{-1} U^2$ and the power of the rotor $N = M\,\omega$. The wind power is treated here as the reference power. From the two above definitions we arrive at the following definition of the efficiency

$$\eta_s = \frac{\omega T}{\rho \frac{U^3}{2} HD} = \frac{\omega D C_T}{2U}. \tag{6}$$

In the above definition ω is the angular velocity, ρ represents the density, and U - the reference velocity. D is the diameter of the rotor, and H is the rotor's height. The steady-state efficiency is frequently referred to as the power coefficient C_P. For the transient case, which is typical for the Savonius rotor operation, one should consider the total energy of the wind within the time interval Δt rather than the instantaneous power. This means that the definition (6) takes the following form now

$$\eta_{\mathrm{t}} = \frac{\omega D \int_{t}^{t+\Delta t} C_{\mathrm{T}}(t)dt}{2U\,\Delta \mathrm{t}} = \frac{\omega D\,\overline{C}_{\mathrm{T}}}{2U} \tag{7}$$

where Δt stands for the time of interest (e.g. one turn). Assuming that the time step $\Delta\tau$ of the transient CFD calculations is constant we can approximate the integral in equation (7) in the following way

$$\int_{t}^{t+\Delta t} C_{\mathrm{T}}(t)\,dt \approx n\,\Delta\tau \frac{1}{n}\sum_{i=1}^{n} C_{\mathrm{T,i}} = \Delta t\ \overline{C}_{\mathrm{T}} \tag{8}$$

where $\overline{C}_{\mathrm{T}}$ represents the arithmetical average $\overline{C}_{\mathrm{T}} = n^{-1}\sum_{i=1}^{n} C_{\mathrm{T,i}}$ and the time of interest Δt (e.g. one revolution) is expressed as $\Delta t = n\,\Delta\tau$. The total number of time steps is denoted here as n. The last definition (7) has an analogical form as the definition (6).

4. Evaluation and comparison criteria

These criteria allow for direct evaluation and comparison of various designs and solutions. As an example of the existing criterion one can recall enstrophy E^* [15]

$$\mathrm{E}^* = \iiint_V \|\mathbf{\Omega}\|^2\,\mathrm{d}V = \iiint_V \frac{1}{2}\left\|\vec{\Omega}\right\|^2\,\mathrm{d}V = \iiint_V \varepsilon^*\,\mathrm{d}V\,, \tag{9}$$

where $\varepsilon^* := 2^{-1}\left\|\vec{\Omega}\right\|^2$ may be again treated as a specific enstrophy. Here $\mathbf{\Omega}$ stands for asymmetrical part of the velocity gradient tensor $\nabla\vec{U}$ and $\vec{\Omega}$ is the vorticity vector. The definition of enstrophy plays important role in theory of turbulence. It determines the rate of dissipation of kinetic energy being a global measure of the dissipation rate and vorticity measure. One can imagine even simpler vorticity measure

$$e^* = \iiint_V \sqrt{2\|\mathbf{\Omega}\|^2}\,\mathrm{d}V = \iiint_V \left\|\vec{\Omega}\right\|\mathrm{d}V\,. \tag{10}$$

Another vorticity measure is defined by means of the integral of the velocity gradient tensor second invariant Q in the following form

$$Q = \iiint_V \mathrm{tr}\left(\nabla\vec{U}\right)^2\,\mathrm{d}V = \iiint_V \left(\mathrm{tr}\,\mathbf{D}^2 - \varepsilon^*\right)\mathrm{d}V\,, \tag{11}$$

where $\mathbf{D}$ stands for symmetrical part of the velocity gradient tensor. The above definition is related to enstrophy defined in equation (9)

$$Q = \iiint_V \mathrm{tr}\,\mathbf{D}^2\,\mathrm{d}V - E^*\,. \tag{12}$$

The so called helicity may be treated as a measure of linkage of vortex lines in the flow. The global helicity is defined as

$$H = \iiint_V \vec{U}\cdot\vec{\Omega}\,\mathrm{d}V\,. \tag{13}$$

Typically, it is better to take advantage of absolute helicity $|H|$

$$|H| = \iiint_V \left|\vec{U} \cdot \vec{\Omega}\right| \mathrm{d}V \tag{14}$$

to avoid cancelling upon integration over considered volume V. An alternative definition of vorticity measure was given by Truesdell

$$W = \iiint_V \frac{\varepsilon^*}{\mathrm{tr}\,\mathbf{D}^2} \mathrm{d}V\,. \tag{15}$$

This measure is combined from two invariants and equals zero for irrotational flow $\left\|\vec{\Omega}\right\| = 0$ and $\mathbf{D} \neq \mathbf{0}$. The measure equals infinity for rotational flow $\left\|\vec{\Omega}\right\| \neq 0$ and $\mathbf{D} = \mathbf{0}$. The former has the largest possible vorticity measure.

Discussed criteria are related to the vortex structures and energy dissipation. These structures are generated by the rotor and may affect the efficiency. There are also different vorticity measure taking advantage of eigenvalues of the velocity gradient tensor.

5. Mesh

The both flow domains, i.e. the rotor and the wind tunnel, were discretised separately. Both domains have an unstructured grid consisting of mostly tetrahedral elements. The total number of elements covering the flow area is about 15 million. There are also special elements around the blades to ensure that flow near a wall is properly resolved. The wall function approach was used to provide near wall boundary conditions for the mean flow. The quality of the grid near the blades may be inspected in terms of y^+ distribution. The average value of y^+ on blades is no greater than 1 for all the time steps.

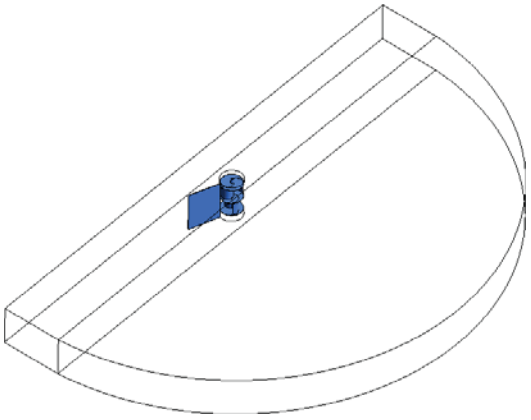

Figure 2. Flow domain.

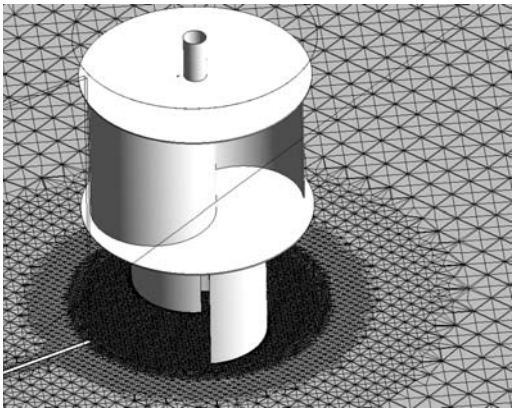

Figure 3. Mesh cross section.

Figure 2 presents global view on the computational domain consists of wind tunnel and cylindrical part of 'far field' surroundings. The mesh can be inspected in figure 3. This figure presents a cross section which is perpendicular to the rotor axis.

6. Results of calculations

Figure 4 presents the torque coefficient C_T distribution as a function of revolution angle. These are results of transient calculations. It has to be pointed out that most of the available data is obtained from

steady-state calculations for two dimensions. The present calculations are fully transient and three-dimensional. The most visible difference between present innovative design and literature data [2, 3, 16, 6] is that there are four peaks visible instead of two. This is because the device consists of two rotors rotated by an angle relative to each other. Additionally, there is a stator directing the flow.

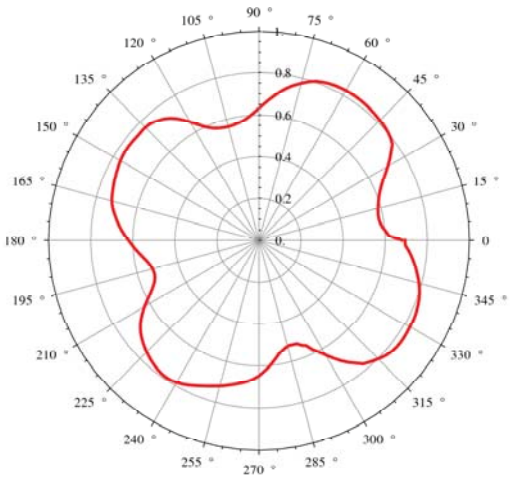

Figure 4. Torque coefficient distribution C_T.

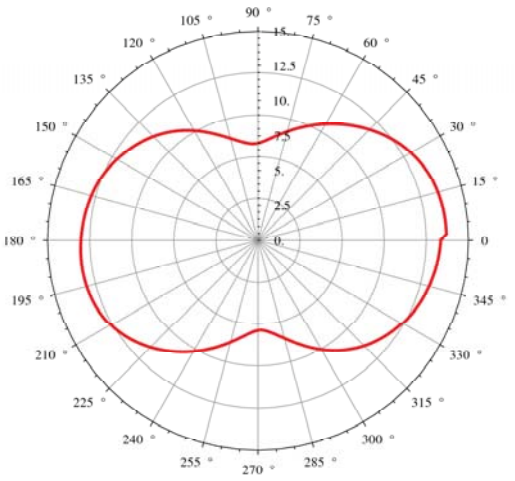

Figure 5. Vorticity measure e^* distribution.

Figure 5 shows distribution of vorticity measure e^* defined by means of equation (10) that can be used to compare various designs indicating the importance of this equation. The time integral of this measure can be used directly to evaluate specific turbine. Furthermore, one can anticipate a relationship between vorticity measure and efficiency of a turbine. It can be expected that the performance of a wind turbine is affected by vortices generated during the rotor revolutions. These vortices are complicated in their nature and dynamically change their configurations and undoubtedly intensities. This may affect pressure distribution around the blades and accordingly the performance of a rotor.

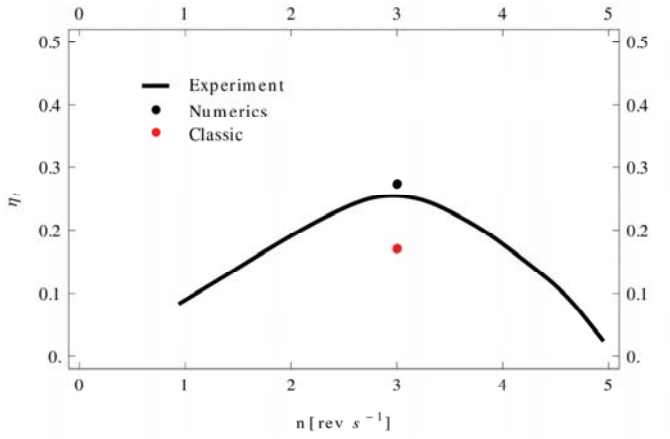

Figure 6. Efficiency comparison η_t.

From the definition (7) it may be deducted that the higher the torque coefficient the more efficient the rotor. The calculated transient efficiency (7) for the innovative design is $\eta_t = 27.3\%$. This value may be easily validated by means of data available in the literature [17] where expected performance of the conventional Savonius rotor for $\lambda = 0.4$ is estimated to be $\approx 17\,\%$. The rotor tip speed ratio λ is defined as

$$\lambda = \frac{\omega D}{2\,\mathrm{U}}. \tag{16}$$

Figure 6 shows the measured efficiency in the wind tunnel for the innovative design (solid line). Black dot shows the numerical prediction of the transient efficiency whereas the red dot represents literature data [17] for the classic Savonius design. Even for low wind speed $6\,\mathrm{m\,s^{-1}}$ the innovative design if far more efficient.

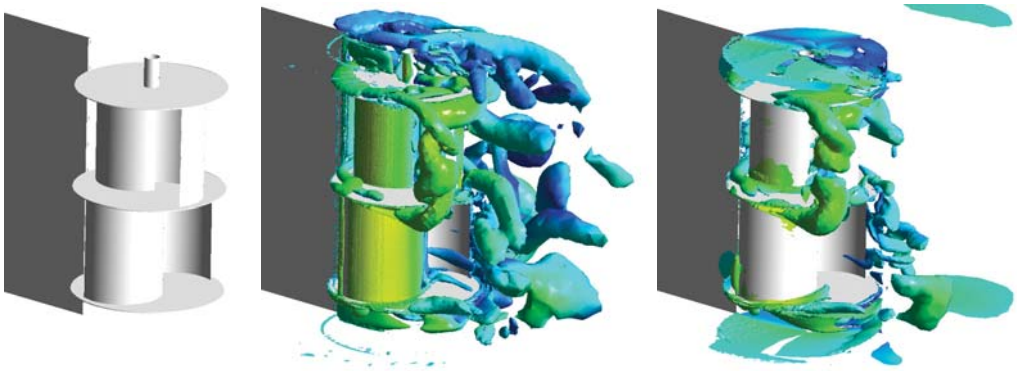

Figure 7. Various vorticity measure distribution.

Figure 7 presents comparison of two example vorticity measure distribution. These are also called vortex cores. In the middle we have $\mathrm{tr}\left(\nabla\vec{U}\right)^2$ distribution which is a part of the integral of the velocity gradient tensor second invariant Q (equation (11)). On the right it is local absolute helicity $\left|\vec{U}\cdot\vec{\Omega}\right|$ being part of global absolute helicity $\left|H\right|$ (equation (14)).

7. Conclusions

- The innovative modification of classic Savonius shows higher efficiency. This is true for wind tunnel experiments at least.
- The increased efficiency is due to presence of the stator which directs the air and makes it possible to take better advantage of its energy.
- It is believed that vortex structures are generated by the rotor and affect the efficiency.
- Several vorticity measure have been proposed allowing for evaluation and comparison of various designs.

8. References

[1] Doerffer P, International patent application PCT/PL2012/000125 and National Patent Application P.397052 – 'Aktywny wiatrak o osi poprzecznej do kierunku wiatru'
[2] Blackwell B F, Sheldahl R E and Feltz L V 1977 Wind tunnel performance data for two- and three-bucket Savonius rotor *Sandia Laboratories Report* SAND 76-0131, 105

[3] Kamoji M A, Kedare S B and Prabhu S V 2008 Experimental investigations on single stage, two stage and three stage conventional Savonius rotor *Int J Energ Res* **32** 877–95
[4] Saha U K, Thotla S and Maity D 2008 Optimum design configuration of Savonius rotor through wind tunnel experiments *J Wind Eng Ind Aerod* **96** 1359–75
[5] Fujisawa N and Gotoh F 1992 Visualisation study of the flow in and around a Savonius rotor *Exp Fluids* **12** 407–12
[6] Nakajima M, Iio S and Ikeda T 2008 Performance of double-step Savonius rotor for environmentally friendly hydraulic turbine *Journal of Fluid Science and Technology* **3** 410–19
[7] Menet J 2008 Prediction of the aerodynamics of a new type of vertical axis wind turbine: the reverse bladed rotor *Proc. of the European Wind Energy Conference*, 2008
[8] Swirydczuk J, Doerffer P and Szymaniak M 2011 Unsteady flow through the gap of Savonius turbine rotor *Task Quarterly* **15**(1) 59–70
[9] Afungchui D, Kamoun B, Helali A and Djemaa A B 2010 The unsteady pressure field and the aerodynamic performances of Savonius rotor based on the discrete vortex method *Renew Energ* **35** 307–13
[10] Ogawa T 1984 Theoretical study on the flow about Savonius rotor *J Fluid Eng-T ASME* **106** 85–91
[11] Mohamed M H, Janiga G, Pap E and Thevenin D 2010 Optimisation of Savonius turbines using an obstacle shielding the returning blade *Renew Energ* **35** 2618–26
[12] Kludzinska K and Swirydczuk J 2012 Unsteady flow through the gap of Savonius turbine rotor *Proc. of the European Congress on Computational Methods in Applied Sciences and Engineering (ECCOMAS 2012)* 2012
[13] Kludzinska K and Swirydczuk J 2012 A numerical analysis of the unsteady flow round a Savonius turbine *Proc. of the XX Polish Fluid Mechanics Conf* 2012
[14] Swirydczuk J and Kludzinska K 2012 Improving Savonius rotor performance by shaping its blade edges *Herald of aeroenginebuilding* **2** 86–90
[15] Tesch K 2013 On invariants of fluid mechanics tensors *Task Quarterly* **17**(3–4) 1000–8
[16] Menet J 2004 A double-step Savonius rotor for local production of electricity: A design study *Renew Energ* **29** 1843–62
[17] Le Gourières D 1980 *Energie éolienne. Théorie, conception et calcul pratique des installations* (Eyrolles)